Friction Modeling and PD Compensation at Very Low Velocities*

Pierre E. Dupont

Eric P. Dunlap

Aerospace and Mechanical Engineering,
Boston University,
Boston, MA 02215

It is a well-known empirical result that stick-slip can often be eliminated from a system by stiffening it. More recently, it has been shown that for a negatively-sloped friction-velocity curve, a frictional lag must be present for machine/controller stiffness to produce this stabilizing effect. In this paper, experiments involving dry and lubricated line contacts of hardened tool steel are described which demonstrate the existence of frictional lag in boundary lubrication. It is also shown that a single-state-variable friction model provides a good representation of the actual friction dynamics. The model and associated parameter values provide a means for computing lower bounds on the machine stiffness and PD gains necessary for steady motion at velocities on the order of microns per second.

1 Introduction

Friction is highly nonlinear at low velocities and poses a considerable challenge to the control of such machines as robots, machine tools and pointing and tracking mechanisms. It is commonly manifested as stick-slip limit cycling in which machine parts alternatively stick and slide with respect to each other. This can occur in position regulation involving integral control where it is known as hunting and also in tracking. In the latter case, it is observed when operating a machine below a critical velocity. While other factors may be important, friction is often the determining factor in the fine-motion fidelity of machines.

Fine-motion fidelity is becoming increasing important in precision engineering where position resolution in nanometers and steady velocities in microns per second are required. For example, in ductile-regime grinding, feed rates on the order of 1 to 100 μm/s produce surface finishes in brittle materials which are comparable to those produced by polishing, but with much greater control of surface shape (Bifano et al., 1991). Similarly, microdrilling (Goto and Kudo, 1992) and machining with single crystal diamond tools (Kobayashi, 1984) involve feed rates in the same range.

Many friction control schemes have been proposed and tested with some success. These include dither, impulsive control (Yang and Tomizuka, 1988; Armstrong-Hélouvry, 1991), stiff PD feedback (Dupont, 1994), model-based feedforward (Armstrong-Hélouvry, 1991) and model-based adaptive control (Canudas De Wit et al., 1991). In addition, learning control provides an alternative to the detailed friction modeling necessary for model-based control (Cetinkunt and Donmez, 1993). Armstrong-Hélouvry et al. (1994) provide a survey of this literature. Their paper also provides a good discussion of the tribology behind friction modeling.

Friction is a very complicated phenomenon which depends on many factors including contact dynamics, surface topology, surface chemistry and lubrication regime. However, it is still possible to approximate the observed friction phenomena for a broad scope of mechanical systems with a dynamic model suitable for controller design and analysis. For example, Armstrong-Hélouvry et al. (1994) propose a seven parameter model in which the parameter values indicate the relative importance of the underlying tribological phenomena.

The analysis of various control schemes is made difficult by the fact that the relative importance of these phenomena is both machine and task dependent. For example, the nanometer-scale displacements encountered in precision engineering are dominated by presliding displacement (Ro and Hubbel, 1993). In this regime, which occurs prior to actual sliding, friction acts as a nonlinear spring. This same phenomenon can be important at velocity reversals (Dahl, 1977; Walrath, 1984; Leonard and Krishnaprasad, 1992).

*This work was supported in part by the National Science Foundation under grants MSS-9112049 and MSS-9302190.

Contributed by the Dynamic Systems and Control Division for publication in the JOURNAL OF DYNAMIC SYSTEMS, MEASUREMENT, AND CONTROL. Manuscript received by the DSCD June 7, 1993; revised manuscript received January 6, 1994. Associate Technical Editor: J. Stein.

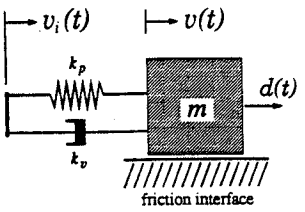

Fig. 1 Sliding system model

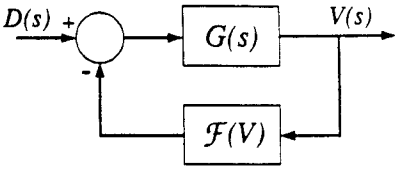

Fig. 2 Block diagram of sliding system model

In unidirectional sliding, frictional memory (describing the lag between changes in velocity and changes in friction force) is important. In fact, the stability of many existing systems can only be explained through consideration of this phenomenon. Two recent papers have brought this to the attention of the control community (Armstrong-Hélouvry, 1993; Dupont, 1994). In the case of PD control, analyses which neglect frictional memory predict that system stability is independent of stiffness and can only be achieved by applying sufficient damping to offset the negative slope of the steady-state friction-velocity curve (Dupont, 1994).

While the fact that friction lags velocity has been reported often in the literature (Bell and Burdekin, 1969; Kato and Matsubayashi, 1970; Antoniou et al., 1976; Bo and Pavelescu, 1982), these efforts have not provided a friction model suitable for the local stability analysis of the unidirectional tracking problem. In particular, the preceding papers are based on stick-slip experiments which are strongly influenced by the dynamics of the stick phase. An exception is (Hess and Soom, 1990) in which carefully controlled velocity oscillations (unidirectional motion) are imposed on a lubricated steel line contact. However, the mixed, elastohydrodynamic and hydrodynamic lubrication regimes are spanned during each velocity cycle. It is therefore questionable whether or not their model is applicable for the micron per second velocities encountered in precision engineering.

The contribution of this paper is to provide the experimental underpinnings for the analytical results involving unidirectional tracking without sticking reported in (Rice and Ruina, 1983) and (Dupont, 1994). Namely, at velocities on the order of microns per second, frictional memory exists in lubricated steel line contacts such as those found in actual machine components. Furthermore, the modeling of frictional memory using a state variable friction law leads to a lower bound on machine and controller stiffness for steady unidirectional sliding.

Assuming constant normal force, the control problem of unidirectional tracking without sticking is idealized by the sliding block depicted in Fig. 1. The input is a velocity source, $v_i(t)$ and the output is the block velocity, $v(t)$. In the remainder of the paper, we will refer to *unidirectional tracking* as the case when $v_i(t) > 0$ and $v(t) > 0$. The coupling between the block and the input is modeled as a spring and dashpot in parallel. The spring represents the stiffness of the transmission while the dashpot models damping in the same. Alternatively, k_p and k_v represent PD gains. A disturbance force on the block, $d(t)$, is also shown.

For a constant input velocity, $v_i(t) = V_0$, the steady-state friction and spring forces cancel and the resulting system can be written in terms of the perturbation velocity, $v(t) - V_0$, and the associated friction force perturbation. This system is best expressed as a mapping from block disturbance force, $D(s) = \mathcal{L}[d(t)]$, to perturbation velocity, $V(s) = \mathcal{L}[v(t) - V_0]$, where $\mathcal{L}[\cdot]$ is the Laplace transform. This relationship is depicted in the block diagram of Fig. 2. The system is composed of a linear block, $G(s)$, where

$$G(s) = \frac{s}{ms^2 + k_v s + k_p} \tag{1}$$

and a block $\mathcal{F}(V(s))$ which is a map from perturbation velocity to perturbation friction force. $\mathcal{F}(V)$ may be linear or nonlinear and with or without memory.

Dupont (1994) describes the necessary relationship between k_p, k_v and $\mathcal{F}(V)$ for local asymptotic stability. In this paper, we present experimental results for modeling $\mathcal{F}(V(s))$ when $v(t)$ is small and nonzero. In the next section, friction modeling is discussed. The experimental procedure is presented in Section 3. Section 4 describes the observed friction for both steady-state sliding and velocity steps. The paper concludes with remarks on friction modeling and the control requirements for stable sliding.

2 Friction Modeling

The velocities associated with the feed rates encountered in precision engineering applications (μm/s) correspond to the lubrication regime known as boundary lubrication. In this regime, the relative velocity between the sliding surfaces is insufficient to develop a separating lubricant film thickness between the surface asperities as occurs in hydrodynamic or elastohydrodynamic lubrication. Solid-to-solid contact dominates the sliding process producing high friction coefficients and wear in the absence of special boundary lubricants. For comparison, friction coefficients in boundary lubrication are usually not much less than 0.1 whereas hydrodynamic lubrication can produce coefficients less than 0.001 (Hamrock, 1986).

For unidirectional motion without sticking, the steady-state friction force is a continuous function of velocity. The slope of this curve depends on the composition of the materials and on the lubricant between them. In general, the friction-velocity curves for hard materials separated by liquid lubricants have negative slopes in the boundary lubrication regime. From a controls viewpoint, a negatively-sloped friction-velocity curve is undesirable because it is destabilizing. A small decrease in velocity causes an increase in the retarding friction force which further reduces velocity. A small increase in velocity causes a decrease in the friction force further increasing the velocity. If this curve alone defined friction behavior then stability could only be achieved through high-gain velocity feedback.

This curve, however, describes only steady-state friction. Sampson et al. (1943) and Rabinowicz (1959) were among the first to note that friction has memory. Its value is not

determined by current velocity alone, but also depends on the history of motion. For constant normal force, this functional relationship for the friction, $f(t)$, can be expressed as

$$f(t) = \mathcal{G}[v(\tau)],\ t - \epsilon < \tau \le t \tag{2}$$

in which v denotes velocity and ϵ is some finite, perhaps small, time interval. In systems prone to stick-slip, frictional memory is a stabilizing effect as it delays the destabilizing steady-state friction behavior.

The equation above describes the evolution of friction between points on the steady-state friction-velocity curve. The literature contains two empirical models for $\mathcal{G}$ which are described below.

2.1 State Variable Friction Models. Research in dynamic friction modeling of rocks has been conducted by geophysicists interested in earthquake prediction (Dieterich, 1979; Ruina, 1980). Their models are referred to as state variable friction models. Recently, the dynamic behavior predicted by these models has been observed in experiments with glass, plastic, wood and teflon on steel (Dieterich, 1991).

For constant normal stress, the general form, including n state variables, θ_i, is given by

$$f(t) = f(v, \theta_1, \theta_2, \ldots, \theta_n) \tag{3}$$

$$\dot{\theta}_i(t) = g_i(v, \theta_1, \theta_2, \ldots, \theta_n),\ i = 1, 2, \ldots, n \tag{4}$$

This form implies that a sudden change in velocity cannot produce a sudden change in the frictional state, θ, but does affect its time derivative. For a single state variable, Ruina (1980) proposed the following friction law.

$$f(t) = f_0 + A \ln (v/V_0) + \theta \tag{5}$$

$$\dot{\theta}(t) = -\frac{v}{L}[\theta + B \ln (v/V_0)] \tag{6}$$

in which θ is the scalar state variable and L is the characteristic sliding length controlling the evolution of θ. The pair (V_0, f_0) corresponds to any convenient point on the steady-state friction-velocity curve. In this case, the steady-state curve is given by

$$f_{ss}(v) = f_0 + (A - B) \ln (v/V_0) \tag{7}$$

and the state variable can be related to the effective age of an asperity junction (Dieterich, 1979).

From (7), $A < B$ indicates a negatively-sloped steady state friction-velocity curve. While the negative slope is destabilizing, the friction dynamics of (5) and (6) ameliorate its effect. The parameter A in (5) is similar to viscous damping. The evolutionary decay of θ described by (6) delays the destabilizing change in friction force with velocity.

Rice and Ruina (1983) and Dupont (1994) have investigated the stability of a system similar to that depicted in Figs. 1 and 2 for the friction law given by (5)–(6) and input velocity $v_i = V_0$. They have shown that, for small perturbations, the block velocity will be asymptotically stable at V_0 if the spring stiffness exceeds a critical value, k_{cr}. Including the dashpot constant, k_v, which can be viewed as the derivative gain in PD control, their result for k_{cr} is given by

$$k_{cr}(V_0) = \frac{B - (A + k_v V_0)}{L}\left[1 + \frac{mV_0^2}{(A + k_v V_0)L}\right] \tag{8}$$

In this case, the resultant machine and controller stiffness, k_p, must exceed k_{cr} for stability.

2.2 Time-Delay Model. Hess and Soom (1990) measured the friction-force response to an oscillating velocity of constant sign in a lubricated line contact. The amplitude of the velocity oscillation was large enough to overlap the mixed, elastohydrodynamic and hydrodynamic lubrication regimes. They found that as the frequency of oscillation increased, the friction-velocity curve became a loop, centered about the steady-state friction curve, whose size increased with frequency. In contrast with boundary lubrication, little if any solid-to-solid contact occurs in the elastohydrodynamic and hydrodynamic lubrication regimes. The observed frictional lag is most likely due to fluid film dynamics.

Hess and Soom modeled this behavior by introducing a time delay in their steady-state equation

$$f(t) = c_0 v(t - \alpha) + \frac{c_1}{1 + c_2 v^2 (t - \alpha)},\ v > 0 \tag{9}$$

where v is velocity, α is the time delay and c_0, c_1, c_2 are positive constants. It has been shown in (Dupont, 1994) that this model does not yield any finite critical stiffness. As long as the delay time, α, is such that the phase shift with respect to velocity is less than π, however, the time-delay friction dynamics promote stability.

The state variable models were specifically developed to model friction at velocities corresponding to boundary lubrication while Hess and Soom's model was formulated to fit a much large range of velocities such as might occur during the slip portion of stick slip. In fact, a time-delay model has recently been used with some success to study the stability of stick-slip limit cycles (Armstrong-Hélouvry, 1993).

The experiments described in the following section were conducted to determine which model, if either, is appropriate for lubricated steel line contacts in boundary lubrication.

3 Experiment Design

A servohydraulic materials testing machine was used with the fixture depicted in Fig. 3 for the friction experiments. The fixture applies normal forces through the two semi-cylindrical riders to the flat test piece. The test piece is attached to a servohydraulic cylinder which moves it in the vertical direction as shown by the arrows. The double-shear design, while averaging the friction at the two interfaces, doubles the friction force sensitivity. As pictured, soft springs are used to maintain a relatively constant normal stress. Load cells, in series with each rider, are used to detect any changes in normal force (±0.6 N) during a trajectory. The load cell at the top of the fixture is attached to a rigid, immobile frame and measures friction force to within ±0.25 N. The friction force load cell was low-pass filtered at 100 Hz. The normal force load cells were filtered at 10 Hz to eliminate noise at 60 Hz. The friction coefficient is obtained by dividing friction force by twice the normal force.

Displacement of the friction interfaces is measured by a

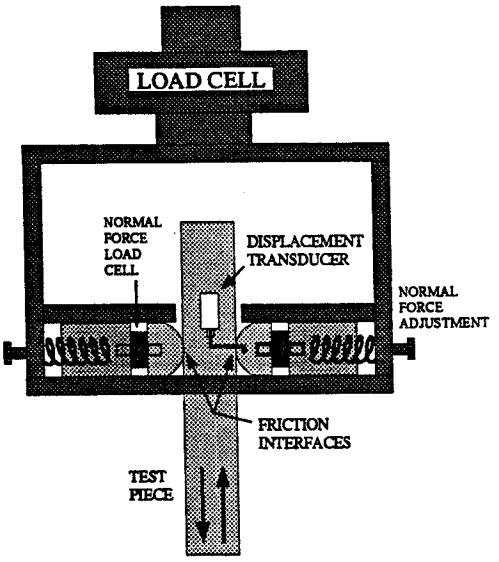

Fig. 3 Double-shear friction fixture. The upper load cell is clamped to a rigid frame while the test piece is clamped to a hydraulic actuator which moves it in the vertical direction.

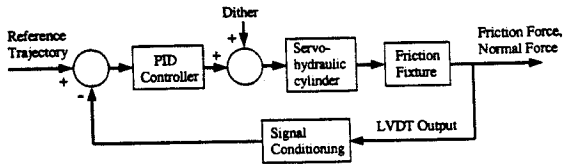

Fig. 4 Block diagram of experiment control system

linear variable differential transformer (LVDT). This transducer is mounted on the unstressed portion of the test piece adjacent to the interfaces. Since displacement is measured very close to the friction interfaces, the measurement excludes most elastic deformation of the fixture and test pieces. The maximum allowable displacement of the actuator, 5 mm, corresponds to that of the LVDT. The resolution and repeatability of the LVDT is ±0.25 μm. The LVDT output is amplified and conditioned using an analog low-pass 100 Hz filter before digitization. The quantization step size is 0.076 μm.

A block diagram of the control loop appears in Fig. 4. A PC (not shown) is used to program reference trajectories and to log the output data consisting of position, friction force and normal force. A digital PID controller operates on position error. The derivative term is approximated using the backward difference method. The integral term is computed as the scaled sum of prior values. The integral gain was set to maintain a given position within ±0.5 μm. There was considerable latitude in selecting the derivative gain. It was set to a small nonzero value to avoid intermittent limit cycling. The proportional gain was set as high as possible to both stabilize and optimize step changes in sliding velocity.

The PID output is combined with a 500 Hz dither sinusoid. A dither amplitude is 0.1 percent of the PID output reduced the effects of servovalve stiction and was not detectable in the unfiltered LVDT output. Thus, the dither is filtered out of the system before reaching the friction interfaces of Fig. 3. The control loop operates at 1 kHz.

Table 1 Composition of boundary lubricant paste

Ingredient	% Weight
Mineral oil	48
Molybdenum disulfide	17
Zinc pyrophosphate	14
Calcium phosphate	13
Ethylene-bis-stearamide	3
Trialuminum phosphate	2
Amorphous silica	1

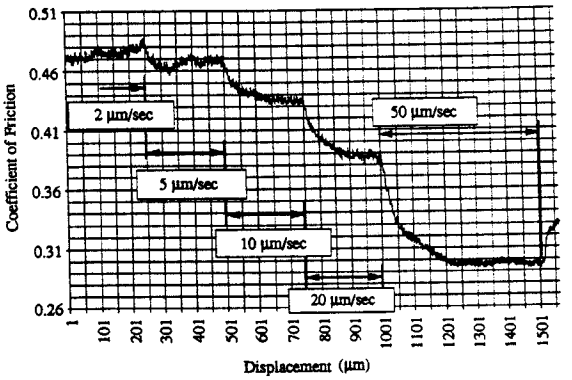

Fig. 5 Collecting steady-state friction data by applying multiple velocity steps during a single pass

4 Experimental Results

Friction was investigated for both steady sliding and step changes in velocity in the range of 1 to 200 μm/s. Three lubrication conditions were studied: dry, paraffin oil with a maximum Saybolt viscosity of 158 and a commercial boundary lubricant paste whose composition is given in Table 1. All samples were made of A.I.S.I. Grade 1 tool steel which was heat treated and oil quenched to a surface Rockwell hardness of 59C.

All tests were conducted with a normal force of 100 N. This value was chosen to avoid excessive wear while also considering the sensitivity of the friction force load cell. The maximum change in normal force observed during any trial was 5 percent. To minimize contamination, separate test and interface pieces were used for the different lubricants. Between each trial, the pieces were lightly polished with 600 grit paper, washed with acetone and lubricated. After lubrication, the surfaces were run in by pulling, then pushing, the test piece through a displacement of 4 mm at 20 μm/s.

4.1 Steady-State Sliding. A steady-state friction versus velocity curve (or Stribeck curve) is assembled from a collection of points, where each point corresponds to the average friction recorded during a constant-velocity trial. The solid-to-solid contact prevalent in boundary lubrication can cause a high wear rate during prolonged sliding. To minimize the effect of accumulated sliding during the progression of steady-state tests, the velocity was stepped every 250 μm of a 3.5 mm tensile displacement of the test piece. The test sequence began with the lowest velocity, reached a maximum midway along the test piece, and then decreased, finishing with the initial minimum velocity. Figure 5 depicts a portion of one trial for paraffin oil. The average friction force for each velocity was computed using the data from the last 50 μm of displacement at that velocity. In this way,

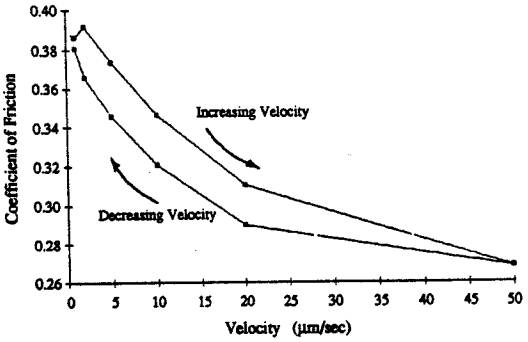

Fig. 6 Steady-state friction for paraffin oil based on eight trials

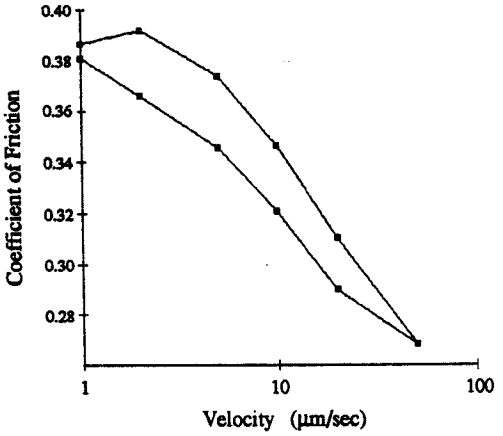

Fig. 7 Steady-state friction for paraffin oil using semi-log axes

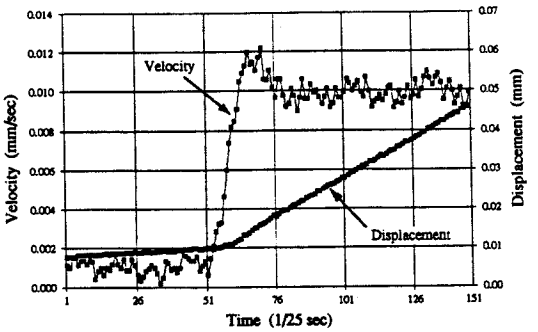

Fig. 8 Displacement and velocity versus time for a typical velocity step

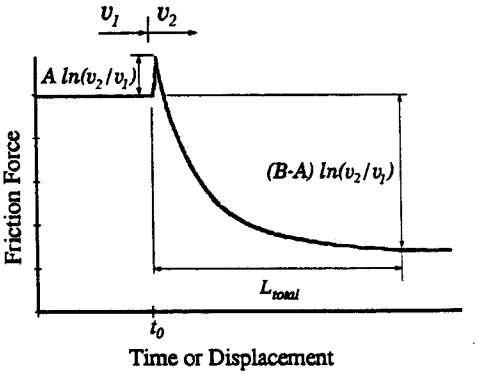

Fig. 9 State variable model parameters from step response

data for seven velocities could be collected twice in a single pass during which the displacement history of the test piece is essentially constant. While the riders (interface pieces) do experience wear during each trial, the effect of this wear appeared to be minimal.

The average of eight trials conducted this way for paraffin oil is shown in Figure 6. Similar to the behavior reported by Hess and Soom (1990), friction following increases in velocity exceeded that following decreases in velocity. This was true for each trial as well as for the average. While this may suggest that steady state was not achieved after 200 μm of sliding, the loop falls well within the standard deviation for the data points of ±20 percent.

Figure 6 is plotted on semi-log axes in Fig. 7. As suggested by (7), $\ln(V)$ provides a reasonable linearization of the steady-state friction-velocity curve.

The boundary lubricant and paraffin oil exhibited a negative dependence of friction on velocity. In dry contact, a negative dependence was observed for new samples which often evolved to a positive dependence after repeated trials without cleaning and repolishing. The reported data is for new samples prepared as described in Section 4.

4.2 Dynamic Friction Behavior. The evolution of friction force between points on the steady-state friction-velocity curve was studied by imposing step changes in velocity at the friction interface. The servohydraulic actuator produced velocity steps with a rise time (10 to 90 percent) of less than 0.5 seconds corresponding to a displacement of less than 5 μm for the velocities considered. A typical velocity step is shown in Fig. 8. While the control loop operates at 1 kHz, the depicted data was logged at 25 Hz. The position data shown is actual LVDT output and the velocity was computed using a 10 point moving average filter and a central difference scheme.

A series of experiments was performed for velocity steps of 1 to 2, 1 to 5 and 1 to 10 μm/s for the three lubrication conditions. The state variable and time delay models were compared with the test data. The results are described below for each model.

4.2.1 State Variable Model. The response of the state variable friction law described by (5) and (6) to a velocity step imposed at time t_0 is shown in Fig. 9. Let the pair (v_1, f_1) correspond to the initial steady state, (v_2, f_2) describe the steady state reached after the velocity jump and f_{max} be the maximum friction force during the transient. The parameters A and B, normalized by normal force N, can be computed from test data using

$$A_\mu = A/N = \frac{f_{max} - f_1}{N \ln (v_2/v_1)} \tag{10}$$

$$B_\mu = B/N = A_\mu - \frac{f_2 - f_1}{N \ln (v_2/v_1)} \tag{11}$$

The exponential decay of the state variable θ following a velocity step is described by

$$\theta = B(e^{-v_2 t/L} - 1) \ln (v_2/v_1) \tag{12}$$

The characteristic sliding length, L, was computed from a least squares fit of the exponential to the data immediately following the velocity step. Determination of B and L was

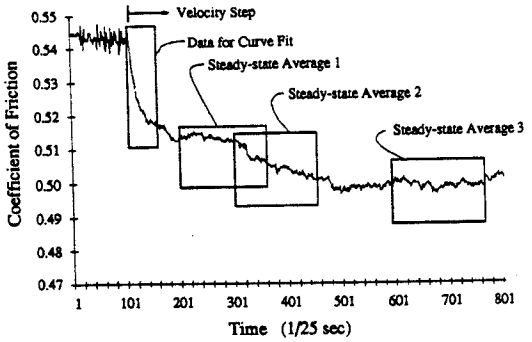

Fig. 10 Curve fitting of exponential decay to typical friction data

Table 2 State variable model parameters for velocity jumps in the range 1–10 μm/s (mean ± standard deviation of the mean)

Parameter	Dry	Paraffin Oil	Boundary lubricant
$A_\mu \times 10^3$	2.8 ± 0.5	0.0*	1.1 ± 0.1
$B_\mu \times 10^3$	9.4 ± 1.1	11.1 ± 2.5	4.0 ± 0.4
L (μm)	64.7 ± 14.3	22.4 ± 4.3	19.2 ± 1.4
k_{cr} (kN/m)	10.2 ± 2.9	49.4 ± 14.5	14.8 ± 2.3

*The magnitude was less than the noise level of the load cell.

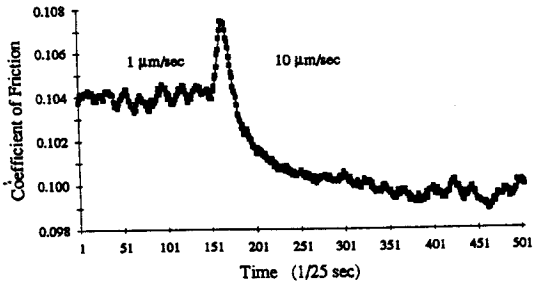

Fig. 11 Single trial showing step response of boundary lubricant

complicated in some cases by the variation in steady-state friction after the step. Three curve fits were made for each jump using values of f_2 computed as averages of 200-point data windows starting 50, 100, and 250 μm after the step. These windows are depicted in Fig. 10. The best fit of the three was selected as the one with the largest coefficient of determination. The coefficient of determination is a statistical parameter which reflects the fit of the data to the calculated exponential. The parameter values obtained in this way were averaged over at least eight trials for each lubricant. The means and standard deviations of the means appear in Table 2.

The instantaneous response to velocity changes, measured by parameter A, was observed in many of the dry and boundary lubricant tests. A single boundary lubricant trial clearly depicts this effect in Fig. 11. For paraffin oil, this effect, if present, was less than the noise level of the load cell. This can be observed in Fig. 5.

Considering the relative magnitude of inertial forces, perturbations about steady sliding are often essentially quasistatic. When this condition is met, and assuming, in the worst case, that $k_v = 0$, the expression for critical stiffness, (8), reduces to

$$k_{cr} = \frac{(B_\mu - A_\mu)N}{L} \tag{13}$$

The critical stiffnesses given by (13) for the three lubrication conditions appear in Table 2. They represent a lower bound on the resultant machine and controller stiffness for asymptotic stability of the linearized system.

4.2.2 Time-Delay Model. The time-delay model predicts a delayed friction step with the same rise time as the velocity-step input. The friction rise time (10 to 90 percent) can be estimated from (12) using the following equation.

$$t_r = \frac{L \ln (9)}{V_2} \tag{14}$$

Friction rise time ranges from over 4 seconds for the boundary lubricant to over 14 seconds for dry sliding. Since these values are considerably larger than the 0.5 second velocity rise time and, in addition, no delay was observed at the start of the step, the time-delay model does not seem appropriate in these circumstances.

5 Conclusions

The reported experiments are the first to demonstrate that frictional memory is presented in lubricated engineering materials operating in boundary lubrication—an important regime for the field of precision engineering. In addition, the existence of an instantaneous viscosity, modeled by A_μ, has not been previously observed for lubricated metals.

The single-state-variable friction model was found to provide a good representation of the velocity-step response. The critical stiffnesses reported in Table 2 represent the resultant stiffness of the machine and controller. The least stiff elements of the experimental apparatus are the fixture and test piece of Fig. 3. Their stiffnesses were measured to be at least 10 MN/m and 1 MN/m, respectively. Comparing these values to the critical stiffnesses, it is clear that, for this system, controller stiffness dominates machine stiffness and thus determines stability.

While it is well known that high-gain P-control with mild D-control can stabilize mechanically-stiff systems with friction, this was, until now, a purely empirical result. If one wanted to implement a system of this type, the only available design methodology was "cut-and-try"—no doubt leading to some overly conservative designs. By combining the stability analyses of (Rice and Ruina, 1983; Dupont, 1994) with the experimental results on frictional memory presented here, we now have an analytical means (still based on friction parameter identification) of sizing mechanical components, selecting transducers and choosing PD gains for stability.

While friction models, such as the state variable laws, are empirical, they are quite effective in controller design and analysis. In order to proceed to predictive friction models, however, it will be necessary to identify the physics underlying frictional memory. The idea of characteristic sliding distances associated with asperity size dates to Rabinowicz (1951). It was motivated in part by the observation that friction increases with time of static contact. It is hypothesized that, due to phenomenon similar to creep, metallic junctions increase in size during contact. A greater force is needed to shear the larger contact regions. The displacement

(characteristic distance) needed to shear the regions is related to junction size. Rabinowicz (1951) proposed that, "Sliding surfaces are equivalent to surfaces in stationary contact for very short times...." Dieterich's (1979) proposal that friction state represents the effective age of asperity junctions is a natural extension of this reasoning. In lubricated contacts, the lubricants determine the surface films and thus influence junction size.

Richardson and Nolle (1976) have shown that in many of the experiments indicating that static friction increases with time of static contact, contact time is directly proportional to loading rate. In their own experiments, they found that loading rate is the critical factor in determining the maximum static friction force. This observation casts doubt on the creep hypothesis of the previous paragraph. More work is needed to determine the dependence of the characteristic sliding distance on surface features, lubricant properties, velocity, and normal force.

Acknowledgment

We deeply appreciate the assistance provided by Dr. David Jablonski and Mr. Roy Foster of the Instron Corporation. We are also grateful to the Instron Corporation for the use of its research laboratory.

References

Antoniou, S., Cameron, A., and Gentle, C., 1976, "The Friction-Speed Relation from Stick-Slip Data," *Wear,* Vol. 36, pp. 235–54.

Armstrong-Hélouvry, B., 1991, *Control of Machines with Friction,* Kluwer Academic Press, Norwell, MA.

Armstrong-Hélouvry, B., 1993, "Stick-Slip and Control in Low-Speed Motion," *IEEE Trans. on Auto. Control,* Vol. 38, No. 10, pp. 1483–1496.

Armstrong-Hélouvry, B., Dupont, P., and Canudas de Wit, C., 1994, "A Survey of Models, Analysis Tools and Compensation Methods for the Control of Machines with Friction," *Automatica,* Vol. 30, No. 7, pp. 1083–1138.

Bell, R., and Burdekin, M., 1969, "A Study of the Stick-slip Motion of Machine Tool Feed Drives," *Proc. Institute Mechanical Engineers,* Vol. 184, Pt. 1, No. 29, pp. 543–60.

Bifano, T., Dow, T., and Scattergood, R., 1991, "Ductile-Regime Grinding: A New Technology for Machining Brittle Materials," ASME *Journal of Engineering for Industry,* Vol. 113, pp. 184–189.

Bo, L. and Pavelescu, D., 1982, "The Friction-Speed Relation and its Influence on the Critical Velocity of Stick-Slip Motion," *Wear,* Vol. 82, No. 3, pp. 277–89.

Canudas De Wit, C., Noel, P., Aubin, A., and Brogliato, B., 1991, "Adaptive Friction Compensation in Robot Manipulators: Low Velocities," *Int. J. Robotics Research,* Vol. 10, No. 3, pp. 189–99.

Cetinkunt, S., and Donmez, A., 1993, "CMAC Learning Controller for Servo Control of High Precision Machine Tools," *Proc. American Control Conference,* San Francisco, CA, pp. 1976–1980.

Dahl, P.R., 1977, "Measurement of Solid Friction Parameters of Ball Bearings," *Proc. of 6th Annual Symp. on Incremental Motion Control Systems and Devices,* University of Illinois, pp. 49–60.

Dieterich, J. H., 1979, "Modeling of Rock Friction: 1. Experimental Results and Constitutive Equations," *J. Geophys. Res.,* Vol. 84 (B5), pp. 2161–2168.

Dieterich, J. H., 1991, "Micro-mechanics of Slip Instabilities with Rate- and State-dependent Friction," (Abstract), Fall Meeting Abstract Volume, Eos, Trans. Am. Geophys. Union, pp. 324.

Dupont, P., 1994, "Avoiding Stick-slip Through PD Control," *IEEE Transactions on Automatic Control,* Vol. 39, No. 5, pp. 1094–1097.

Goto, F. and Kudo, S., 1992, "Measurement of the Plastically Deformed Domain Caused by Microdrilling in CdS Single Crystal," *Precision Engineering,* Vol. 14, No. 4, pp. 243–245.

Hess, D. and Soom, A., 1990, "Friction at a Lubricated Line Contact Operating at Oscillating Sliding Velocities," ASME *Journal of Tribology,* Vol. 112, No. 1, pp. 147–52.

Kato, S. and Matsubayashi, T., 1970, "On the Dynamic Behavior of Machine-tool Slideway—1st Report, 2nd Report," *Bull. Jap. Soc. Mech. Eng.,* Vol. 13, No. 55, pp. 170–88.

Kobayashi, A., 1984, "Ultra-Precision Machining of Plastics," *Proc. SPIE Production Aspects of Single Point Machined Optics,* San Diego, CA, SPIE Vol. 508, pp. 31–36.

Leonard, N. and Krishnaprasad, P., 1992, "Adaptive Friction Compensation for Bi-directional Low-velocity Position Tracking," *Proc. 31st CDC,* Tucson, AZ, pp. 267–273.

Rabinowicz, E., 1951, "The Nature of the Static and Kinetic Coefficients of Friction," *Journal of Applied Physics,* Vol. 22, No. 11, pp. 1373–79.

Rice, J., and Ruina, A., 1983, "Stability of Steady Frictional Slipping," ASME *Journal of Applied Mechanics,* Vol. 50, No. 2, pp. 343–49.

Richardson, R. and Nolle, H., 1976, "Surface Friction Under Time-Dependent Loads," *Wear,* Vol. 37, No. 1, pp. 87–101.

Ro, P., and Hubbel, P., 1993, "Model Reference Adaptive Control of Dual-Mode Micro/Macro Dynamics of Ball Screws for Nanometer Motion." ASME JOURNAL OF DYNAMIC SYSTEMS, MEASUREMENT, AND CONTROL, Vol. 113, pp. 103–108.

Ruina, A., 1980, "Friction Laws and Instabilities: A Quasistatic Analysis of Some Dry Frictional Behavior," Ph.D. dissertation, Division of Engineering, Brown University.

Sampson, J., Morgan, F., Reed, D., and Muskat, M., 1943, "Friction Behavior During the Slip Portion of the Stick-Slip Process," *J. of Applied Physics,* Vol. 14, No. 12, pp. 689–700.

Walrath, C., 1984, "Adaptive Bearing Friction Compensation Based on Recent Knowledge of Dynamic Friction," *Automatica,* Vol. 20, No. 6, pp. 717–27.

Yang, S., and Tomizuka, M., 1988, "Adaptive Pulse Width Control for Precise Positioning Under the Influence of Stiction and Coulomb Friction," ASME JOURNAL OF DYNAMIC SYSTEMS, MEASUREMENT, AND CONTROL, Vol. 110, pp. 221–227.